

## Proton-Proton Scattering Near the Interference Minimum and the Shape Parameter\*

J. E. BROLLEY, JR., J. D. SEAGRAVE, AND J. G. BEERY

Los Alamos Scientific Laboratory, University of California, Los Alamos, New Mexico

(Received 30 April 1964)

At a laboratory proton energy of 382.43 keV,  $p$ - $p$  scattering exhibits nearly complete destructive interference, and the  $s$ -wave phase shift may be determined from the location,  $E_{\min}$ , of the minimum in the cross section for  $90^\circ_{\text{e.m.}}$  scattering, with comparable precision. A determination of the phase shift at  $E_{\min}$  to one part in  $10^3$  may be combined with recent Wisconsin results between 1.4 and 3 MeV to give information about the shape-dependent term in the effective-range expansion. Measurements have been made of the relative cross section at six energies near that of the minimum, using a scattering chamber with annular slits of  $90^\circ$  vertex angle and a group of coincident pairs of silicon particle detectors. The energies of the data points were established by a radio-frequency, time-of-flight absolute velocity gauge, with an uncertainty of less than 50 eV. The scattering chamber was differentially pumped upstream and downstream. The operating pressure was 0.3 Torr, and the upstream energy loss of about 150 eV was measured directly by noting the offset of the  $F^{19}$  ( $p, \alpha\gamma$ ) $O^{16}$  resonance when hydrogen was present in the chamber between the velocity gauge and a differentially pumped  $CF_4$  gas target. The minimum was relocated at  $E_{\min} = 382.43 \pm 0.20$  keV, and the corresponding  $s$ -wave phase shift with respect to the "electric" wave functions including vacuum polarization is found to be  $\delta_0^s = 0.25501 \pm 0.00020$  rad. The shape-dependent parameter inferred from these results is significantly positive,  $P = +0.028 \pm 0.014$ . This may be considered strong evidence in favor of one-pion-exchange effects in the  $s$ -wave interaction.

### INTRODUCTION

ONE of the oldest problems of nuclear physics is the scattering of protons by protons. Significant advances in the experimental aspects of this problem occurred in the 1930's with the introduction of particle accelerators in the MeV range. The predictions of Coulomb scattering in the Mott form were not consistent with the experimental results.<sup>1-4</sup> Moreover, the empirical knowledge indicated an unexpectedly low probability of scattering at  $90^\circ_{\text{e.m.}}$  in the vicinity of 400-keV laboratory energy of the incoming proton.<sup>5-16</sup>

Concomitant theoretical explication<sup>17,18</sup> provided a picture of destructive interference between a postulated nuclear force field and the Coulomb field. The interference effect is conspicuous in the summary presentation of Fig. 1. A simple analytic representation of the energy dependence of  $90^\circ_{\text{e.m.}}$  scattering which takes cognizance of Coulomb scattering in all angular momentum states plus nuclear scattering in the singlet  $s$  state is given in Eq. (1).

$$\sigma_{\text{e.m.}}(90^\circ) = \left(\frac{2e^2}{mv^2}\right)^2 \left(1 - 2\frac{\sin\delta_0 \cos\epsilon}{\eta} + \frac{\sin^2\delta_0}{\eta^2}\right). \quad (1)$$

Here  $\delta_0$  is the phase shift generated by the nuclear force

\* Research performed under the auspices of the U. S. Atomic Energy Commission.

<sup>1</sup> W. H. Wells, Phys. Rev. **47**, 591 (1935).

<sup>2</sup> M. G. White, Phys. Rev. **47**, 573 (1935); **49**, 309 (1936).

<sup>3</sup> M. A. Tuve, N. P. Heydenburg, and L. R. Hafstad, Phys. Rev. **50**, 806 (1936).

<sup>4</sup> L. R. Hafstad, N. P. Heydenburg, and M. A. Tuve, Phys. Rev. **53**, 239 (1938).

<sup>5</sup> Experimental data from many sources is conveniently summarized for  $E_p \leq 7.5$  MeV in Ref. 6. For a general perspective, the reviews of Refs. 7-15 may be consulted.

<sup>6</sup> *Charged Particle Cross Sections*, Los Alamos Report LA-2014, 1957, edited by N. Jarmie and J. D. Seagrave (unpublished).

<sup>7</sup> J. D. Jackson and J. M. Blatt, Rev. Mod. Phys. **22**, 77 (1950).

<sup>8</sup> L. Hulthen and M. Sugawara, in *Handbuch der Physik*, edited by S. Flügge (Springer-Verlag, Berlin, 1957), Vol. 39, p. 1.

<sup>9</sup> M. H. MacGregor, M. J. Moravcsik, and H. P. Stapp, Ann. Rev. Nucl. Sci. **10**, 291 (1960).

<sup>10</sup> M. J. Moravcsik and H. P. Noyes, Ann. Rev. Nucl. Sci. **11**, 95 (1961).

<sup>11</sup> G. Breit, Rev. Mod. Phys. **34**, 766 (1962).

<sup>12</sup> J. L. Gammel and R. M. Thaler, Progr. Elem. Particle Cosmic Ray Phys. **5**, 97 (1960).

<sup>13</sup> R. J. N. Phillips, Repts. Progr. Phys. **22**, 562 (1959).

<sup>14</sup> M. A. Moravcsik, *The Two-Nucleon Interaction* (Oxford University Press, Oxford, 1963).

<sup>15</sup> R. Wilson, *Nucleon-Nucleon Interaction* (John Wiley & Sons, Inc., New York, 1963).

<sup>16</sup> M. A. Preston, *Physics of the Nucleus* (Addison-Wesley Publishers, Inc., Reading, Massachusetts, 1962), Chaps. 2, 5, and Appendix B.

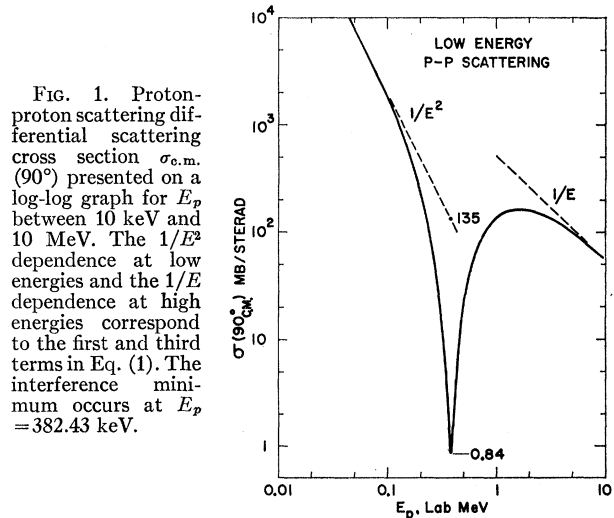


FIG. 1. Proton-proton scattering differential scattering cross section  $\sigma_{\text{e.m.}}(90^\circ)$  presented on a log-log graph for  $E_p$  between 10 keV and 10 MeV. The  $1/E^2$  dependence at low energies and the  $1/E$  dependence at high energies correspond to the first and third terms in Eq. (1). The interference minimum occurs at  $E_p = 382.43$  keV.

<sup>17</sup> G. Breit, E. U. Condon, and R. D. Present, Phys. Rev. **50**, 825 (1936).

<sup>18</sup> G. Breit, H. M. Thaxton, and L. Eisenbud, Phys. Rev. **55**, 1018 (1939).

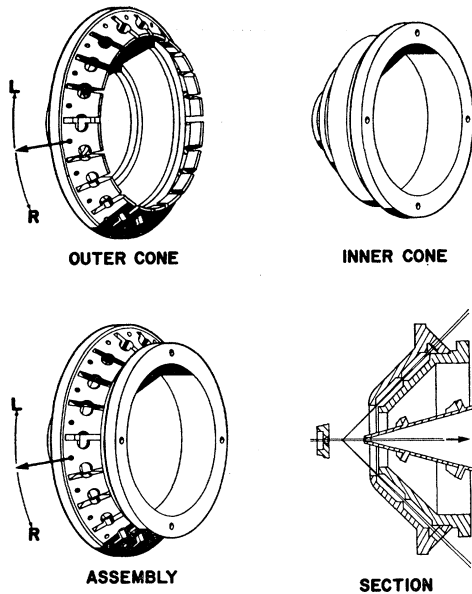


FIG. 2. Annular slit system for the scattering chamber, showing the inner and outer cones, their assembled state, and a cross section showing their position in the scattering chamber of Fig. 4. The labels  $L$  and  $R$  indicate the left- and right-handed semislit edge division about the plane of symmetry indicated by the arrow.

field,  $\eta = e^2/\hbar v = 0.1581 (E_{\text{MeV}})^{-1/2}$ ,  $\hbar$  is Planck's constant over  $2\pi$ ,  $v$  is the laboratory velocity of the incoming proton,  $m$  its mass, and  $e$  its charge. The phase shift  $\delta_0$  increases and the Coulomb parameter  $\eta$  decreases with increasing energy. For simplicity, we have introduced  $\epsilon = \delta_0 - \eta/n2$ , since in the vicinity of the minimum, which occurs at an energy such that  $\sin \delta_0 \approx \eta \approx 0.25$  rad,  $\cos \epsilon \approx 1$ .

This phenomenon has been utilized by Cooper, Frisch, and Zimmerman<sup>19</sup> to determine  $\delta_0$  experimentally. Using a differentially pumped scattering chamber equipped with proportional counters and a Van de Graaff accelerator to supply the proton beam they determined the minimum to be at  $E_{\text{min}} = 383.9 \pm 1.5$  keV. Using a more precise relationship between the phase shift and the observed minimum than the one just stated, they computed the value  $\delta_0 = 0.2527 \pm 0.0011$  rad. The accuracy of their determination was limited in part by the stability of the accelerator and the precision of its energy standardization. The latter was based on observations of  $(p, \gamma)$  resonances in  $\text{Li}^7$  and  $\text{F}^{19}$ .

Attainment of considerably higher precision in  $E_{\text{min}}$  and  $\delta_0$  was the first objective of the present work. Moreover, we sought to establish the values of certain parameters in the effective-range theory.<sup>7</sup> This theory describes  $s$ -wave nucleon-nucleon scattering by relating  $\delta_0$  to these parameters. The theory is not convergent above approximately 10 MeV.<sup>20</sup> As applied to proton-

proton scattering it takes the form given by Eq. (2):

$$C^2 k \cot \delta_0 + \frac{\hbar(\eta)}{R} = -\frac{1}{a} + \frac{1}{2} r_0 k^2 - P r_0^3 k^4 + \dots, \quad (2)$$

using the conventional symbols of Jackson and Blatt.<sup>7</sup> The scattering length  $a$  and the effective range  $r_0$  provide some characterization of the nuclear force field independent of its detailed shape. The shape parameter  $P$  is considerably more sensitive to the model used for the nuclear potential. By way of qualitative illustration we note that for reasonable values of  $a$  and  $r_0$ ,  $P$  is negative for the square and Gaussian well shapes, nearly zero for the exponential shape and definitely positive for the Yukawa well. Until the present work, the sign of  $P$  had not been definitely established, though the numerical value was felt to be less than 0.1. Some hard-core potential models that have been used to describe nucleon-nucleon scattering also predict a negative shape parameter. Evidently the evaluation of  $P$  would be of some interest.

In principle, the effective-range theory determines  $P$  if  $\delta_0$  can be measured at three different energies. However, Heller<sup>21</sup> has shown that the energy intervals between measurements should be as great as possible and that one of the measurements should be as close to zero energy as possible. The measurements on the angular distribution of proton-proton scattering by Knecht, Messelt, and Dahl<sup>22,23</sup> at 1.397, 1.855, 2.425, and 3.037 MeV are not sufficient by themselves. When used in conjunction with a measurement of comparable precision at the interference minimum, they should permit the calculation of  $P$ .

Full utilization of the precision of the experimental data requires consideration of the effect of vacuum polarization on the effective-range theory. This has been done by Heller.<sup>21</sup> Inclusion of the vacuum polarization in the effective-range theory gives rise to Eq. (3):

$$C^2 k [(1 + 2\chi_0) \cot \delta_0^E - \tau_0] + \frac{\hbar(\eta)}{R} + \frac{I_0(\eta)}{R} = -\frac{1}{a} + \frac{1}{2} r_0 k^2 - P r_0^3 k^4, \quad (3)$$

with the notation given by Heller.  $\delta_0^E$  is the nuclear scattering phase shift referred to the total *electric* scattering of Coulomb *plus* vacuum polarization;  $\tau_0$  is the phase shift for zero angular momentum scattering by the vacuum polarization field. Equation (3) forms the basis for the present investigation. The analysis of Heller shows that the phase shift inferred from a measurement of the interference minimum is increased approximately

<sup>19</sup> L. Heller, Phys. Rev. **120**, 627 (1960).

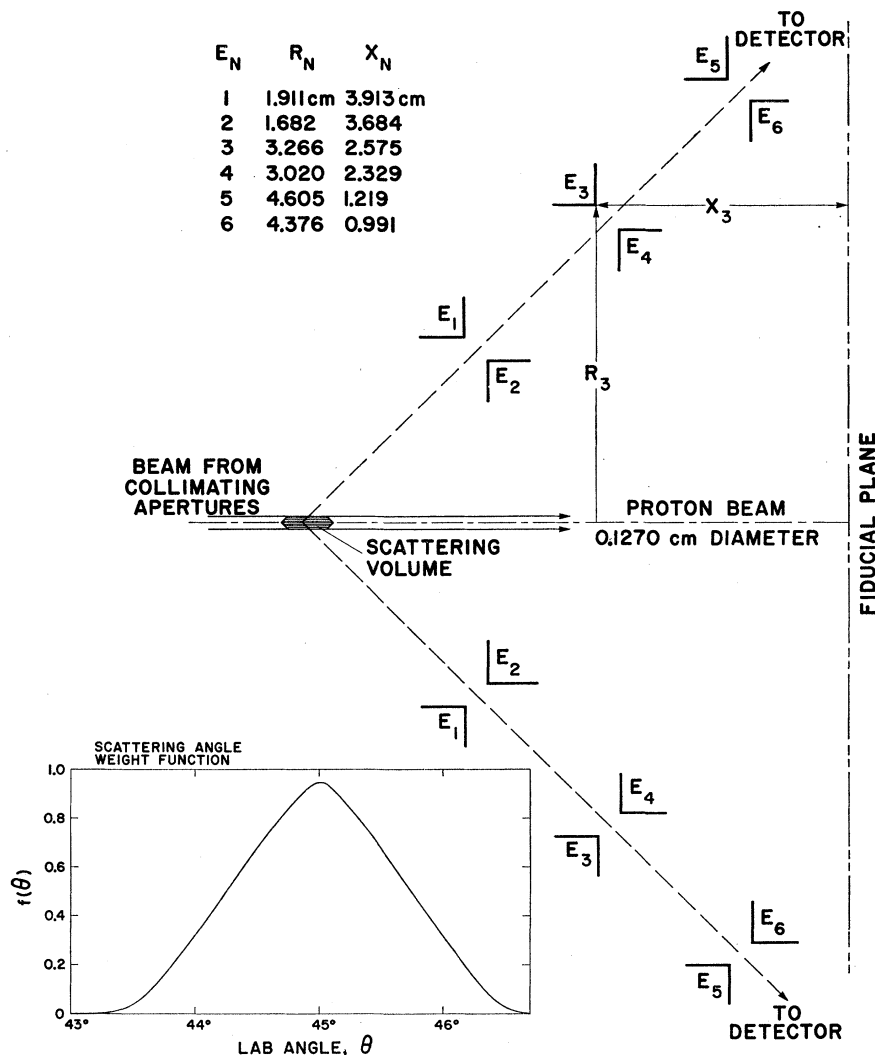
<sup>19</sup> D. I. Cooper, D. H. Frisch, and R. L. Zimmerman, Phys. Rev. **94**, 1209 (1954).

<sup>20</sup> H. P. Noyes and D. Y. Wong, Phys. Rev. Letters **3**, 191 (1959).

<sup>21</sup> D. J. Knecht, S. Messelt, E. D. Berners, and L. C. Northcliffe, Phys. Rev. **114**, 550 (1959).

<sup>22</sup> D. J. Knecht, S. Messelt, and P. Dahl, University of Wisconsin (unpublished).

FIG. 3. Diagram and table showing the location of the annular slit edges  $E_N$ : their radial dimensions  $R_N$  and axial dimensions  $X_N$  from a fiducial plane. Shown at the lower left is the weighting function which meet the coincidence requirement of  $90^\circ$  between scattered and recoil protons passing into the associated detectors.



$\frac{1}{2}\%$  when vacuum polarization is considered. Also for fixed values of  $a$  and  $r_0$ , the calculated value of  $E_{\min}$  was found to shift upward about 0.7 keV with the inclusion of vacuum polarization. These refinements of the theory and the estimate<sup>24</sup> that a redetermination of  $E_{\min}$  with an accuracy of  $\pm 0.3$  keV would permit inference of the value of  $P$  with an uncertainty of  $\pm 0.02$  provided the motivation for the present experiment.

**EXPERIMENTAL DESIGN**

Prior to the design of this experiment it was necessary to establish permissible limits on the various parameters of the apparatus. A preliminary computer code including both relativity and vacuum polarization effects was developed by Heller. The sensitivity of the expected experimental results to imprecision and spread of various parameters was explored with this code. Some of the salient results of this investigation were: statistical

<sup>24</sup> L. Heller (private communication).

uncertainties of about 1% in counting at five energy points, spaced 10 keV apart in the vicinity of the minimum, were acceptable, and finite scattering and azimuthal angular intervals of  $\Delta\theta = 2^\circ$ ,  $\Delta\phi = 5^\circ$  were satisfactory. The energy points were required with an accuracy of  $\pm 100$  eV to permit a sufficiently precise determination of  $E_{\min}$ .

**SCATTERING CHAMBER**

Since  $90^\circ_{\text{c.m.}}$  scattering corresponds to both the scattered and recoil protons emerging from the reaction volume at  $45^\circ$  to the beam axis, it is possible to construct a conical slit system to accommodate both particles. Such a slit system can be fabricated with a high degree of precision. Since it includes particles in all azimuthal planes, it provides greater data acquisition rate than the conventional arrangements of the same resolution. A cross section of the slit system is shown in Fig. 2 together with the beam ingress and egress apertures of the

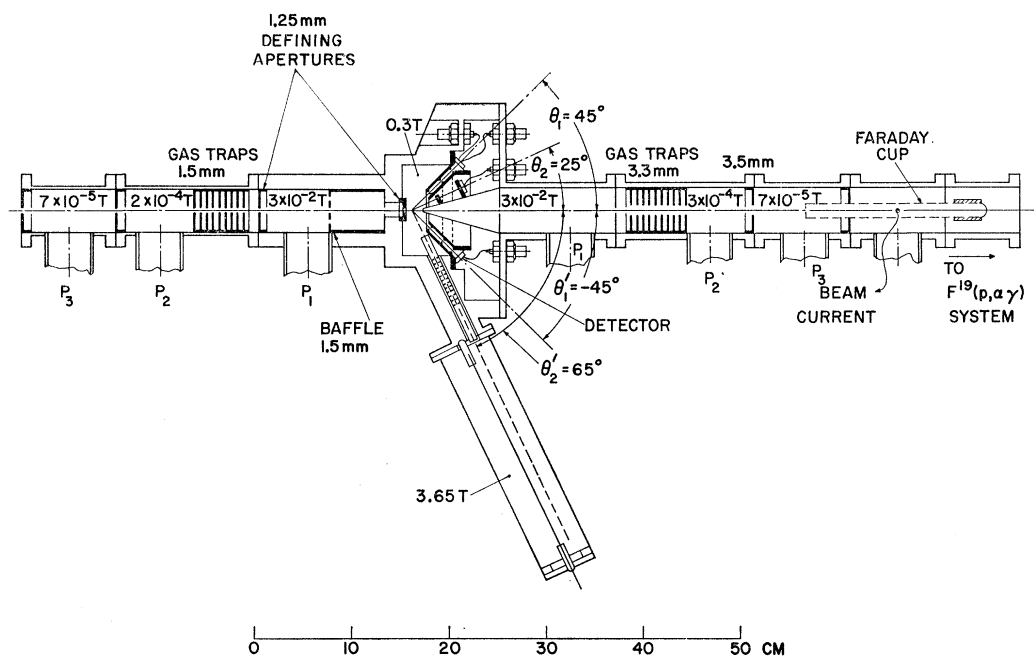


FIG. 4. Differentially-pumped scattering chamber for  $p$ - $p$  scattering measurements at  $\theta_{lab} = 45^\circ$ . The ring-slit system is shown heavily inked. Connection to three separate pumping systems  $P_1$ ,  $P_2$ , and  $P_3$  is indicated. Pressures are given in Torr (T). In addition to the apertures shown, an ancillary aperture of 2.5-mm diam was located 1.98 m upstream of the final beam ingress aperture, at the upstream end of the velocity gauge.

proton scattering chamber. Angular definition in the  $\theta$  coordinate is determined by the two extreme slits. Pairs of silicon detectors in electrical coincidence, diametrically placed on the exit side of the outer cone, delimit an angular spread somewhat smaller than that which prevails for noncoincidence or singles counting. This is easily demonstrated graphically by observing permissible scattered and recoil trajectories with a triangle whose  $90^\circ$  vertex lies in the proton beam. Such a procedure also indicates that the reaction volume contributing to coincidences is smaller than that which would supply singles counts. A perspective of the inner and outer cones and their assembled state is also given in Fig. 2. Some of the more important dimensions are indicated in Fig. 3 together with a plot of the angular weight function. This function, which comes from the calculations of Gursky and Heller,<sup>25</sup> gives the relative degree of participation of the various scattering angles contributing to a coincidence observation. The full width at half-maximum is  $1.6^\circ$ .

It was possible to encompass the whole range of azimuthal angles ( $0 \leq \phi \leq 2\pi$ ) with available silicon detectors by locating them at twenty equal intervals, equally spaced. The apertures were of such a width as to be completely spanned by the sensitive area of the silicon detectors. The azimuthal boundaries of each counting area must be very accurately known. Fabrication of the slits which set the azimuthal boundaries

was made precise and simple by virtue of the geometry of the coincidence requirement. Each counter and its homolog lie about a plane containing the proton beam axis. The coincidence condition requires only one boundary at each counter, both boundaries being in a plane parallel to the central scattering plane. The azimuthal interval is not constant but is very accurately known over the counting area. The configuration of the  $\Delta\phi$  semislits is also shown in Fig. 2.

Ten pairs of silicon detectors were peripherally located on the outer cone of the slit system. Considerable difficulty was encountered in retaining ten pairs that would continue to register 100–200-keV protons satisfactorily in the hydrogen environment. Only four pairs survived to the final data acquisition phase. Constant quality control was maintained on those that survived as described below. All pairs of counters used had delayed as well as prompt coincidence circuitry in order to measure accidental coincidences.

The slit and counter assembly was housed in a differentially pumped scattering chamber shown in Fig. 4. Principal definition of the proton beam entering this chamber was by means of the defining apertures indicated and another ancillary aperture approximately 2 m upstream. The unscattered proton beam emerged from the scattering chamber through a port located adjacent to the scattering volume, in the conical structure at the rear of the chamber. Thus, the beam lost relatively little energy in the scattering chamber which was maintained at a pressure of  $\frac{1}{3}$  Torr. The beam then could proceed

<sup>25</sup> M. L. Gursky and L. Heller (to be published).

either to a shielded and biased Faraday cup, strapped with magnets, or to another experimental apparatus designed for the observation of the reaction  $F^{19}(p,\alpha\gamma)O^{16}$ . Charge deposited in the cup was measured by a vibrating reed electrometer and integrator circuit.

Much of the hydrogen gas in the chamber exhausted through the aforementioned ports. However, additional pumping from another port, not shown in Fig. 4, was required. The gas was continuously purified prior to admission into the scattering chamber. The coincidence requirement plus simultaneous accidental counting with the delayed-coincidence circuit further minimized the effect of scattering by impurities. Hydrogen was supplied via four proportional counters, only one of which is shown in Fig. 4. A pressure of 3.65 Torr was maintained in the counters. The gas issued from counters through gas traps that permitted a pressure drop of 3.3 Torr to be maintained. Protons scattered at laboratory angles of 65 or 70° entered the proportional counters through the gas traps. The companion protons at 25 or 20° were detected by silicon counters mounted on the exit cone. This coincidence system was originally conceived as being a monitoring system. The scattering minimum we sought could be inferred<sup>7</sup> from observation of the ratio of 90°<sub>c.m.</sub> scattering to scattering at some forward angle. However, the performance of this system was somewhat unsatisfactory and it was relegated to otiose status after serving during initial alignment studies.

All components of the chamber were made of steel to provide magnetic shielding and gold or nickel plated to preclude corrosion. Some parts were hardened where necessary. All critical dimensions were known to an accuracy of  $\pm 0.0005$  cm.

#### ACCELERATOR

As the source of protons we selected the Los Alamos Cockcroft-Walton accelerator, which could supply an adequate current of magnetically analyzed protons in the desired energy range, 300–410 keV. Considerable work was done on this machine to reduce the various types of modulation and instability present. The principal energy modulation, arising from 2-kc ripple in the high-voltage power supply, was reduced by applying a signal, appropriately phased, from the 2-kc motor-generator supply to the insulated “ground” end of a 600-kV filter capacitor.

Energy stability was the paramount accelerator consideration, since the value of the energy of the beam was measured independently of the accelerator equipment, as will be described in the next section. A common error signal controlled two types of regulators. The error signal was obtained by comparing the current in a shielded precision resistor stack, bridging the high-voltage supply, with a standard current, using conventional potentiometric null methods. The slow regulator, which employed motor-driven variable transformers,

was speeded up to the point of hunting, and a second fast regulator was constructed in the form of a corona triode drawing about 0.5 mA of ion current directly from the high-voltage terminal. The source impedance was about 10 M $\Omega$ . The load was controlled by a non-linear circuit which operated primarily on the fast component of voltage spikes and fluctuations, to preclude hunting by the slow system. Under very favorable conditions the voltage could be regulated to about one part in 10<sup>6</sup>, but nominal regulation was more nearly one part in 10<sup>4</sup>, or 40 V in 400 kV. As indicated in the schematic diagram of Fig. 6, the beam proceeded up the vertical accelerator and was turned and analyzed by a magnet and slit system. After the analysis it passed through an ion-optical system consisting of electrostatic displacement and lens components.

#### ENERGY DETERMINATION

The principal problem in designing this experiment was whether the absolute energy of the beam could be measured with the accuracy required, nearly one part in 10<sup>4</sup> for each data point. Theory was of no help here, although we were assured that the residual ripple, and thermal motion of the gas<sup>26</sup> would not have serious consequences, when they were taken into account. We chose to measure the beam velocity directly in terms of length and frequency, quantities which are susceptible to very precise determination. This was achieved by constructing an absolute velocity gauge which measured the beam time of flight in a radio-frequency cavity, very similar in principle to the device constructed and evaluated by Altar and Garbuny<sup>27</sup> and Shoupp, Jennings, and Jones<sup>28</sup> in 1948. A detailed description of this instrument will be published separately.<sup>29</sup> The principle is indicated in Fig. 5. There is a field-free drift space along the axis. At either end, small gaps permit the field of the passing protons to excite the cavity at its characteristic frequency. If the time of flight within the drift space is an odd half-multiple of the cavity period, the exit gap will excite oscillations of opposite phase, and a null, or condition of minimum energy storage, will obtain. In the representation of Fig. 5, the beam is shown modulated in discrete packets. If there are  $N$  packets of charge in length  $L$  between gaps, and the cavity and modulation frequency is  $f$ , then the null will occur when the particle velocity  $v=2fL/(2N-1)$ , and its energy  $E_N$  is given by the relation

$$E_N = \frac{1}{2}m_0c^2 \left[ \frac{2fL}{(2N-1)c} \right]^2 \left\{ 1 + \frac{3}{4} \left[ \frac{2fL}{(2N-1)c} \right]^2 + \dots \right\}. \quad (4)$$

<sup>26</sup> Even the zero-point motion of the hydrogen molecule produces random spreading of the energy of scattering several times the precision required for the *mean* energy. We are indebted to C. Critchfield for calling our attention to this question.

<sup>27</sup> W. Altar and M. Garbuny, Phys. Rev. **76**, 496 (1949).

<sup>28</sup> W. E. Shoupp, B. Jennings, and W. Jones, Phys. Rev. **76**, 502 (1949).

<sup>29</sup> J. D. Seagrave, J. E. Brolley, Jr., and J. G. Beery, Rev. Sci. Instr. (to be published).

In Eq. (4),  $c$  is the velocity of light, and  $m_0$  the particle rest mass. The quantity in square brackets is the ratio of particle velocity to that of light, and the second term in the expansion is the first-order relativistic correction. Our instrument was constructed with  $L=125$  cm, and  $f$  in the range 70 to 74 Mc for the energy of interest. Modulation of the proton beam at a frequency  $f$  was accomplished by applying an rf voltage of frequency  $\frac{1}{2}f$  to modulator plates between the accelerator and the bending magnet, as shown in Fig. 6. The source of this voltage was a conventional crystal oscillator, frequency multiplier and power amplifier system. The frequencies of the various crystals used for different energy measurements were in the 9-Mc region. They were regularly measured by direct counting with a calibrated instrument, and were always known to one part per million. Other techniques for frequency measurement were also employed as checks.

Typical response curves were about 200 eV wide at half-maximum, and all energy points could be determined to  $\pm 40$  eV or less. The precision was limited by ripple, instability, and drift of the accelerator. The average drift during a typical data run of about 30 min in the scattering experiment was about 100 eV. Measurements were made at six different energies, corresponding to five frequencies between 70 and 74 Mc with the value  $N=11$ , and a lower energy point at the highest frequency and the next value  $N=12$ .

In order to assure ourselves that we understood the operation of this instrument, we remeasured one of the  $F^{19}(p,\alpha\gamma)O^{16}$  resonances which is close to this lowest energy point, and found  $E_R=340.45\pm 0.04$  keV. This may be compared with the previously accepted value,<sup>30</sup>  $E_R=340.5\pm 0.2$  keV. This measurement was made with a voltage-offset technique whereby the machine could be held at the energy determined by the velocity gauge and the nearby resonance examined as a function of the offset voltage of a few kilovolts. This facility also per-

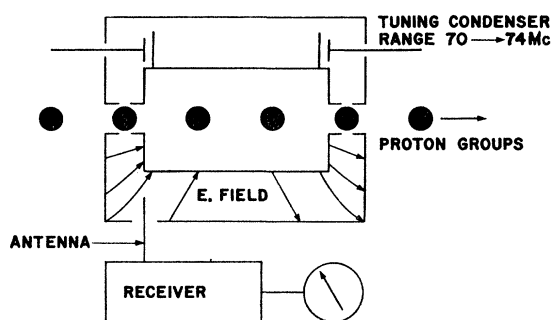


FIG. 5. Schematic diagram of the principle of the absolute velocity gauge. Proton beam is shown chopped into discrete packets. The situation shown is the condition for a *maximum* excitation of the cavity, with  $N=4$ . In use, the beam velocity is adjusted for a *minimum* excitation at the operating frequency, and one gap is between packets when a packet just passes through the other gap.

<sup>30</sup> J. B. Marion, Rev. Mod. Phys. 33, 139 (1961).

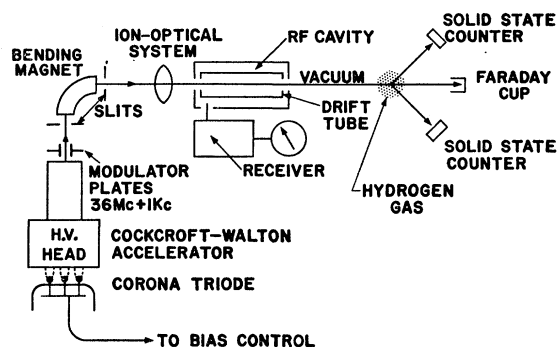


FIG. 6. Schematic diagram of the main components of apparatus used in the  $p$ - $p$  scattering experiment.

mitted a direct measurement of the energy loss in the gas-filled scattering chamber by noting the shift in the apparent location of the fluorine resonance when hydrogen was let into the chamber. This over-all check permitted comparison with the results of energy loss calculated from the material in Whaling's compendium<sup>31</sup> and pressure data in the several stages of differential pumping, supplemented by ancillary measurements of the pressure drops in the multiple gas traps. Typical upstream energy loss was 150 eV.

#### DATA ACQUISITION

Each group of observations at a particular energy was arranged to spread over two days of operation in such a way that each day measurements were made at two energies until the cycle was closed. While operating at any particular energy numerous individual runs of approximately one-half-hour duration were made, involving measurement of energy, charge, pressure, and temperature. Frequent measurements of the modulation frequency and occasional retuning of the cavity were performed as required. True random coincidence factors for the coincidence circuitry were determined with the aid of random noise sources built from similar silicon detectors. At the beginning of each day's operation, coincident pulse-height spectra were obtained for each of the detectors in operation, and the discriminator setting for each channel was selected and recorded on each spectrum photograph by applying a pulser simultaneously to the inputs of coincident pairs, and increasing the pulse height until the discriminator fired and passed on the pulse to the analyzer, where a second photograph was superimposed. Thus, for each counter in use, we obtained a daily record such as is shown in Fig. 7, on which basis the operating point could be selected, or an unacceptable counter revealed.

Since we had found it necessary to abandon the forward-angle monitor counters, and rely on the Faraday cup for charge measurement, the collected charge then became a basic datum. We verified that substantial

<sup>31</sup> W. Whaling, in *Handbuch der Physik*, edited by S. Flügge (Springer-Verlag, Berlin, 1959), Vol. 34, p. 193.

TABLE I. Experimental results for *p-p* scattering near the interference minimum. The columns tabulated are (a) the mean energy at target center, (b) the uncertainty of the mean energy determination, (c) the crystal oscillator frequency controlling excitation of the velocity gauge, (d)–(f) net counts in channels 1–3, (g) the total counts  $N_3$  recorded at each energy, (h) the expected standard deviation for  $N_3$ , (i) an error estimate based on control of experimental conditions, (j) the standard deviation from internal consistency of data, (k) the current integrator count for each run ( $K = \times 1000$ ), and (l) the mean ratio of counts per integrator count.

(a) $E_p$ keV	(b) $\Delta E$ keV	(c) $f/8$ Mc	(d) $n_1$	(e) $n_2$	(f) $n_3$	(g) $N_3$	(h) $N^{-1/2}$ %	(i) $e_x$ %	(j) $e_{int}$ %	(k) $Q$	(l) $n(3)/Q$
337.66	$\pm 0.04$	9.24967	1317 2772	1249 2510	1317 2678	11 843	0.92	0.13	1.62	25K 50K	52.42
362.48	$\pm 0.06$	8.74983	1097 1100 1056 1116	1095 1059 1068 1061	1185 1113 1072 1074	13 096	0.88	0.20	0.95	67K 67K 67K 67K	16.28
372.83	$\pm 0.03$	8.87431	1155 1151 1289 1174	1152 1168 1169 1267	1060 1138 1150 1135	14 008	0.85	0.28	1.50	110K 110K 110K 110K	10.61
383.48	$\pm 0.06$	8.99946	883 1243 1248 1183 622 554	948 1128 1134 1164 591 600	872 1135 1127 1090 593 526	16 641	0.78	0.23	1.13	110K 140K 140K 140K 70K 70K	8.280
394.25	$\pm 0.05$	9.12481	1135 1115 1125 1162	1185 1137 1134 1163	1140 1087 1137 1085	13 605	0.86	0.13	(0.79)	110K 110K 110K 110K	10.31
405.17	$\pm 0.04$	9.24973	1174 1133 1156 1138	1140 1089 1182 1138	1118 1145 1216 1110	13 739	0.85	0.13	0.85	70K 70K 70K 70K	16.36

changes in the operating pressure about the normal point did not affect current monitoring. We further verified that the effect of beam heating of the target gas was not significant in the region of nominal current, 0.5  $\mu$ A. The reproducibility of the current integrator was checked frequently by noting the counts in unit time when the input was supplied with constant current from a standard cell whose voltage under load was checked before and after the experiment. Checks were repeatable within  $\pm 0.1\%$ .

Pressure was monitored by a variety of means, and drifts were recorded. The primary pressure measurement before and after each run was made with an oil manometer and cathetometer.

The recorded data for each run were then the following: pressure, temperature, high-voltage potentiometer readings before and after the data run, and the coincidence and accidental counts in each channel, together with the number of integrator counts for the run. Integrator and frequency checks were noted as often as appeared desirable. The data points were corrected by the true accidental rate (usually a few percent), and pressure and temperature factors (also a few percent) were applied to reduce the data to standard conditions, namely 0.307 Torr and 20°C. Included was an empirical correction for the effect of expansion of gas into the chamber. It was assumed that the actual drift of ma-

chine energy between velocity gauge checks was opposite to the change in potentiometer setting required to restore the machine energy to the gauge point. The potentiometer had been arranged to give the nominal energy in keV directly in terms of its numerical reading in millivolts. The mean energy during the run was taken as the calculated gauge point plus half the measured drift (usually under 100 eV), and half the drift was used as an estimate of the energy uncertainty due to experimental conditions. The upstream energy loss was subtracted, and the mean energy for the run tabulated.

RESULTS

The consolidation of our measurements is given in Table I. The detectors were located every 18° in azimuth, but only three of the ten pairs participated in the final

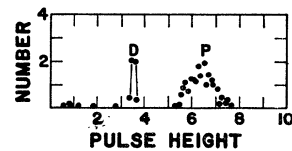


FIG. 7. Pulse-height spectrum for 180-keV protons (P) observed at  $\theta_{lab} = 45^\circ$  in coincidence with a similar particle, from *p-p* scattering at 360 keV. Superimposed is a pulse marker corresponding to the discriminator setting (D) selected for this channel.

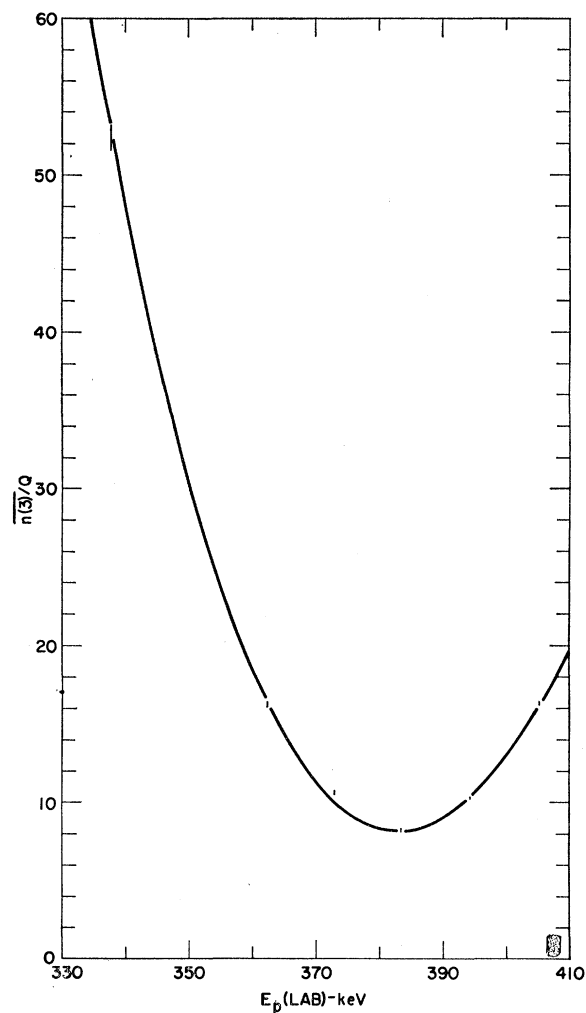


FIG. 8. Comparison of relative counting rate  $\overline{n(3)}/Q$  from Table I as a function of proton energy  $E_p$  near the interference minimum with best theoretical fit (omitting point at 373 keV) in which the theoretical cross section has been folded with the finite geometrical resolution. Fit shown gives  $E_{\min}=383.43\pm 0.13$  keV, with  $a=-7.80$  F and  $r_0=2.65$  F. Best fit with all six points gives a curve indistinguishable from the other with the linewidth employed.

data.<sup>32</sup> This data has been subjected to exhaustive statistical analysis by our colleagues Gursky and Heller, details of which will be found in their paper.<sup>25</sup> The goodness of fit may be seen qualitatively in Fig. 8, which shows the relative counting rate as a function of energy, compared with the theoretical rate, with all geometrical factors folded into the theoretical expression. It was

<sup>32</sup> The counts for those three channels are labeled in Table I  $n_1$ ,  $n_2$ , and  $n_3$ ; the corresponding azimuth angles, measured clockwise from the vertical, looking upstream, were 27–207°, 135–315°, and 99–279°. A fourth pair of counters at azimuth angles 81 and 261° was carried through the entire data acquisition phase, passing all electrical tests. It was found consistently low in counts by 11%, and could not be included in the analysis, since making allowance for the uncertainty in location of a possible dead spot in one counter vitiated the statistical advantage of including the data.

TABLE II. Singlet “electric”  $p$ - $p$  scattering phase shifts derived by Noyes from measurements at the University of Wisconsin (Refs. 22 and 23) between 1.4 and 3.0 MeV, together with the present results (Ref. 25) at the interference minimum. The “electric” phase shifts  $\delta_0^E=K_0-\tau_0$  differ from the values of  $K_0$  tabulated by Noyes (Ref. 34) by the vacuum polarization phase shift  $\tau_0$  given by Heller (Ref. 21).

Lab proton energy, $E_p$ (MeV)	Singlet phase shift, $\delta_0^E$ (rad)	Vacuum polarization phase shift, $\tau_0$ (rad)
$0.38243\pm 0.00020$	$0.25501\pm 0.00020$	$-1.83\times 10^{-3}$
$1.397\pm 0.00125$	$0.68621\pm 0.00026$	$-1.49\times 10^{-3}$
$1.855\pm 0.00166$	$0.77398\pm 0.00037$	$-1.39\times 10^{-3}$
$2.425\pm 0.00218$	$0.84406\pm 0.00024$	$-1.31\times 10^{-3}$
$3.037\pm 0.00273$	$0.89035\pm 0.00035$	$-1.24\times 10^{-3}$

found that the goodness-of-fit parameter  $\chi^2_{\min}$  has the expected value  $n-3$  for  $n$  data points only if the data at  $E_p=372.83$  keV were omitted.<sup>33</sup> Since the 373-keV set of data is suspected to contain spurious random counts arising from accelerator sparking subsequently eliminated, the set could be legitimately dropped, but since it passed the experimental tests at the time, as further data which led to locating the trouble did not, it is reasonable to consider including that set with a weight reflecting the added uncertainty. In a supplementary analysis, the weight was decreased for the 373-keV set until the  $\chi^2$  sum was constrained to the expected value. This led to an uncertainty increased to 0.15 keV, which value we have assigned to the 5-point mean value determination. Thus we adopt  $E_{\min}=383.43\pm 0.15$  keV for the final values of the location of the minimum and the net experimental uncertainty. The calculated value<sup>25</sup> of the phase shift  $\delta_0^E=0.25501\pm 0.00020$  rad at  $E_p=383.430$  keV. (Note added in proof. More refined analysis<sup>25</sup> including the acceptable spread in values of  $P$  requires increasing the uncertainty of  $E_{\min}$  to  $\pm 0.20$  keV, to include the ambiguity in the theoretical curve.)

The phase-shift datum from the present experiment may now be collated with the results of the experiments of Knecht, Messelt, and Dahl.<sup>23</sup> Their data do not yield the singlet phase shift directly. To extract useful phase shifts it is necessary to take cognizance of the vacuum polarization as well as the contributions of the triplet- $p$  phases. Noyes<sup>34</sup> has calculated the triplet- $p$  phases to what is believed to be an adequate degree of precision, and using these  $p$  phases and vacuum polarization theory, he has computed the  $\delta_0$  phases. The corresponding “electric” phase shifts  $\delta_0^E$  are given in Table II.

<sup>33</sup> The data at 373 keV were taken just before an accelerator breakdown (sparking in the motor-generator) forced abandoning later data and making a major repair. Though the data were repeatable at the time, it may be that electromagnetic disturbances undetected in noise led to occasional prompt coincidences in one channel at a time. After the repair, the possible source was monitored, and the rest of the data is known to be free of this effect.

<sup>34</sup> H. P. Noyes (private communication); and Phys. Rev. Letters 12, 171 (1964). We are indebted to Professor Noyes for communicating these values prior to publication.



Gursky and Heller<sup>25</sup> have utilized the complete set of phase shifts to compute the shape parameter from the effective range theory and found  $P=0.028\pm 0.014$ . This value of  $P$  discriminates against a number of simple models<sup>35-38</sup> and computational artifices such as the square, Gaussian, and exponential wells and favors the Yukawa well. A recent calculation by Noyes<sup>34</sup> including the one-pion-exchange contribution leads to the value  $P=+0.024$ , in excellent agreement with our result. Other models,<sup>20,39-42</sup> quantitative in varying degree, also predict positive shape parameters.

<sup>35</sup> G. Breit and W. Bourcius, Phys. Rev. **75**, 1029 (1949).

<sup>36</sup> H. Feshbach and E. Lomon, Phys. Rev. **102**, 891 (1956).

<sup>37</sup> H. P. Noyes, in *Nuclear Forces and the Few Nucleon Problem*, edited by T. C. Griffith and E. A. Power (Pergamon Press, Inc., London, 1960), p. 39.

<sup>38</sup> H. P. Noyes, Phys. Rev. **130**, 2025 (1963).

<sup>39</sup> D. Y. Wong and H. P. Noyes, Phys. Rev. **126**, 1866 (1962).

<sup>40</sup> M. Cini, S. Fubini, and A. Stanghellini, Phys. Rev. **114**, 1632 (1959).

<sup>41</sup> J. K. Perring and R. J. N. Phillips, Nucl. Phys. **23**, 153 (1961).

<sup>42</sup> P. Signell and R. Yoder, Phys. Rev. **122**, 1897 (1961).

#### ACKNOWLEDGMENTS

It is a pleasure to record our indebtedness to L. Heller for invaluable counsel in the design of the experiment, and to him and M. Gursky for discussion of their analysis of the data. R. Hiebert designed and modified for our special requirements much of the electronic equipment and was very helpful in trouble-shooting. A. Shopp and G. Bjarke of the Los Alamos Electrical Standards Laboratory contributed generously of their equipment and services. We also thank E. Graves and R. W. Davis for making available several hundred hours of accelerator time, and J. Dion and A. Tegtmeier for extricating us from some difficult accelerator maintenance problems. R. Booth and M. Gibson skillfully operated the accelerator and equipment. Finally, the mechanical design and fabrication of the scattering chamber and velocity gauge were made possible by the help of W. Borckenhagen, T. Carroll, and E. Galvin.